

YALE PEABODY MUSEUM

P.O. BOX 208118 | NEW HAVEN CT 06520-8118 USA | PEABODY.YALE. EDU

JOURNAL OF MARINE RESEARCH

The *Journal of Marine Research*, one of the oldest journals in American marine science, published important peer-reviewed original research on a broad array of topics in physical, biological, and chemical oceanography vital to the academic oceanographic community in the long and rich tradition of the Sears Foundation for Marine Research at Yale University.

An archive of all issues from 1937 to 2021 (Volume 1–79) are available through EliScholar, a digital platform for scholarly publishing provided by Yale University Library at <https://elischolar.library.yale.edu/>.

Requests for permission to clear rights for use of this content should be directed to the authors, their estates, or other representatives. The *Journal of Marine Research* has no contact information beyond the affiliations listed in the published articles. We ask that you provide attribution to the *Journal of Marine Research*.

Yale University provides access to these materials for educational and research purposes only. Copyright or other proprietary rights to content contained in this document may be held by individuals or entities other than, or in addition to, Yale University. You are solely responsible for determining the ownership of the copyright, and for obtaining permission for your intended use. Yale University makes no warranty that your distribution, reproduction, or other use of these materials will not infringe the rights of third parties.



This work is licensed under a Creative Commons Attribution-NonCommercial-ShareAlike 4.0 International License.
<https://creativecommons.org/licenses/by-nc-sa/4.0/>



Buoyancy-driven circulation as horizontal convection on β -plane

by Nobuo Suginohara¹ and Shigeaki Aoki²

ABSTRACT

The nature of the steady buoyancy-driven circulation is investigated using multi-level numerical models. An ocean which extends over the northern and southern hemispheres is forced by cooling in a confined region and heating in the rest of the ocean through the sea surface. As is already known, the circulation and associated thermal structure strongly depend upon the effect of the vertical diffusivity. This nature of the buoyancy-driven circulation is found in the thermodynamic balance. The vertical diffusion plays an essential role in the whole ocean domain. In counterbalancing the vertical diffusion, the horizontal advection at the deepest levels and the vertical advection in the rest of the interior region plays a dominant role. Thus, horizontal transport of cold water from the convective (cooling) to the diffusive (heating) region occurs mainly in the lowest part of the deep water. It is a natural consequence of predominance of the vertical diffusion that the buoyancy-driven circulation has a significant vertical shear well below the thermocline; the Stommel and Arons pattern for the deep circulation tends to be confined in the lower part of the deep water.

Details of a set of alternating zonal jets along the equator and associated meridional circulation are obtained and discussed, and dependence on diffusivity and viscosity is also discussed.

1. Introduction

The ocean general circulation may be divided into wind-driven and thermohaline circulations in terms of the forcing agencies, although superposition is not possible due to nonlinearity of the system. Progress on the development of a theory for the thermohaline circulation has lagged behind that for the wind-driven circulation. This can be attributed to a number of the fundamental features of the thermohaline circulation which inhibit both observations and analysis of the appropriate systems of equations. These include the extreme asymmetry between the downwelling and upwelling branches, the extremely long time scales and essential nonlinearity of the thermodynamic balance. The asymmetry is a fundamental characteristic of the thermally driven circulation in the ocean or analogous laboratory systems (Stommel,

1. Department of Earth and Planetary Physics, Faculty of Science, University of Tokyo, Yayoi, Bunkyo-ku, Tokyo 113, Japan.

2. National Research Institute for Pollution and Resources, 16-3, Onogawa, Tsukuba-shi, Ibaragi 305, Japan.

1962; Rossby, 1965). Sinking motions occur in very confined regions, and in fact are very rarely observed in the ocean. Consider an ocean where heat enters and leaves through the sea surface. It is in effect added by conduction and eliminated by convection. Thus, the asymmetry is maintained by relative efficiencies of heat transfer by convection to that by conduction, and the thermocline is a natural consequence of the thermohaline circulation. Heat is carried horizontally from the diffusive (heating) to the convective (cooling) region. This certainly indicates the importance of nonlinearity in the thermodynamic balance.

There are several forerunners of the present work. Among them the following works are particularly informative. Bryan (1987) demonstrated strong dependence of circulation on the effect of vertical diffusivity in a general circulation model, i.e., with increasing diffusivity, the thermocline deepens and the circulation becomes stronger. Colin de Verdière (1988) studied the thermohaline circulation within the context of planetary geostrophy, and demonstrated detailed dependence on the diffusivity although a convincing explanation for its physics was not given. Suginohara and Fukasawa (1988) (hereafter referred to as SF) intended to interpret and improve the far-reaching idea of the deep circulations of Stommel and Arons (1960). Using a multi-level numerical model, they studied an ocean initially filled with a homogenous warm water driven by a prescribed cold water formation inside the ocean in the southern part of the southern hemisphere. Set-up of deep circulation is clearly demonstrated in their model as follows. Density currents which tend to conserve potential vorticity play an essential role in establishing the thermal structure. Cooling of the whole ocean starts with introduction of the cold water from the formation region into the deepest part of the ocean in the equatorial and eastern boundary regions by Kelvin wave-type density currents. The cold water along the eastern boundary extends westward as a Rossby wave-type density current setting up the interior poleward flow, and hits the western boundary to form a northward flowing boundary current in the northern hemisphere. Only then does the western boundary current cross the equator. Cooling of the rest of the ocean basin is accomplished by upwelling in the interior and also along the coasts. An important result of their model is that the thermal structure is formed even in the deep water as the cold water is mixed with surrounding warm waters during the introduction, and the resulting circulation at a steady state has a significant vertical structure such that the maximum upwelling in the interior occurs in the mid-depths. Thus, they indicate that the Stommel and Arons pattern tends to be confined in the lower part of the deep water. Also they pointed out that cooling in the equatorial region occurs in a different way from off the equator, i.e., higher vertical mode motions dominate forming a set of alternating zonal jets along the equator, since motions in the equatorial region are free from the geostrophic vorticity constraint. However, the thermal structure obtained in their model cannot be directly compared with that of the real ocean, because the upper part of the model ocean is poorly resolved.

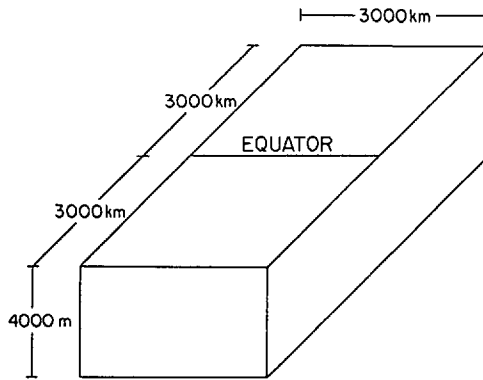


Figure 1. Schematic view of the model ocean.

Thus, the works of Bryan, Colin de Verdière and SF indicate that it is necessary to investigate the nature of the thermohaline circulation more thoroughly by taking finer vertical resolution for both the upper and lower parts of the ocean as well as fine resolution in the horizontal directions. And the new findings of SF such as a set of alternating zonal jets along the equator and the significant vertical shear in circulation in the deep water need to be clarified.

In the present paper, using multi-level numerical models constructed in the way discussed above, a thorough discussion of the steady thermohaline circulation will be given though effects of salinity are not considered. We regard the buoyancy-driven circulation as horizontal convection on a β -plane. An ocean which extends over the northern and southern hemispheres is forced by differential heating through the sea surface. Cooling in the confined region and uniform heating in the rest of the ocean is imposed. The uniform and broad heating will help to avoid complexities which originate from the differential heating distributed over the whole ocean surface. Several case-studies are made to understand dependence on diffusivity and viscosity. A case where the cold water is formed inside the ocean as in SF is also studied, and an intuitive picture of the basic dynamics of the horizontal convection will be presented. Only the steady state solution will be discussed because the essential features of set-up of deep circulation have already been given in SF.

2. Model

We consider a rectangular ocean which extends over the southern and northern hemispheres as shown in Figure 1. The latitudinal width is 3000 km and the longitudinal width is 6000 km. The ocean has a flat bottom and is 4000 m deep. We use a rectangular coordinate system on an equatorial β -plane with x eastward, y northward and z vertically upward from the mean sea surface level. Let u , v and w be the components of velocity in the x , y and z directions, respectively, P the pressure

and ρ the density. The equation of motion and the hydrostatic relation under the Boussinesq approximation are

$$\begin{aligned} \frac{\partial u}{\partial t} + u \frac{\partial u}{\partial x} + v \frac{\partial u}{\partial y} + w \frac{\partial u}{\partial z} - fv &= -\frac{1}{\rho_0} \frac{\partial P}{\partial x} + A_v \frac{\partial^2 u}{\partial z^2} + A_H \nabla_H^2 u, \\ \frac{\partial v}{\partial t} + u \frac{\partial v}{\partial x} + v \frac{\partial v}{\partial y} + w \frac{\partial v}{\partial z} + fu &= -\frac{1}{\rho_0} \frac{\partial P}{\partial y} + A_v \frac{\partial^2 v}{\partial z^2} + A_H \nabla_H^2 v, \\ 0 &= -\frac{\partial P}{\partial z} - \rho g, \end{aligned}$$

and the continuity equation is

$$\frac{\partial u}{\partial x} + \frac{\partial v}{\partial y} + \frac{\partial w}{\partial z} = 0,$$

where A_v and A_H are coefficients of the vertical and horizontal eddy viscosity, respectively, ρ_0 the mean density over the whole depth, g the acceleration of gravity, ∇_H the horizontal gradient operator, and $f (= \beta y)$ the Coriolis parameter. The equation of density under the assumption that density and temperature have a linear relation is

$$\frac{\partial \rho}{\partial t} + u \frac{\partial \rho}{\partial x} + v \frac{\partial \rho}{\partial y} + w \frac{\partial \rho}{\partial z} = \frac{K_v}{\delta} \frac{\partial^2 \rho}{\partial z^2} + K_H \nabla_H^2 \rho,$$

where K_v and K_H are coefficients of the vertical and horizontal eddy diffusivity, respectively. And δ , a convective adjustment parameter used to maintain a stable stratification, is defined by

$$\delta = \begin{cases} 1, & \text{if } \partial \rho / \partial z \leq 0 \\ 0, & \text{if } \partial \rho / \partial z > 0. \end{cases}$$

At the sea surface, the density flux

$$\frac{\gamma_s}{\rho_0 C_v} (\rho^* - \rho)$$

is imposed, where C_v is the specific heat at constant volume, ρ the density at the sea surface and $\gamma_s = 50 \text{ cal } (\text{°C cm}^2 \text{ day})^{-1}$. The reference density, ρ^* is a function only of latitude and is distributed such that cooling takes place in the confined region (Fig. 2). The maximum value of ρ^* at the southern edge of the basin is 30.0 in σ_t units, and the uniform value outside the formation region is 24.0 in σ_t units. On the side walls and bottom the normal gradient of density is zero so that there is no density flux across these boundaries.

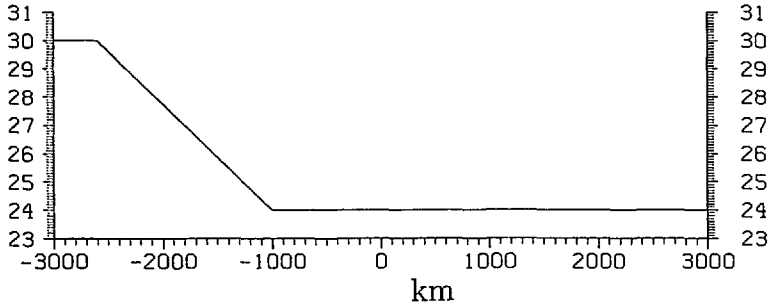


Figure 2. Meridional distribution of the reference density, ρ^* in σ_t units.

At the sea surface the wind stress is not taken into consideration. Friction is considered at the bottom (see SF). The side walls are the no-slip boundaries.

As the initial condition a weakly stratified ocean is considered to suppress density currents with large amplitude as discussed in SF. It should be remarked that a steady state solution does not depend on the initial condition at least within our parameter range.

The numerical method used in this study is that of SF. It should be remarked that a

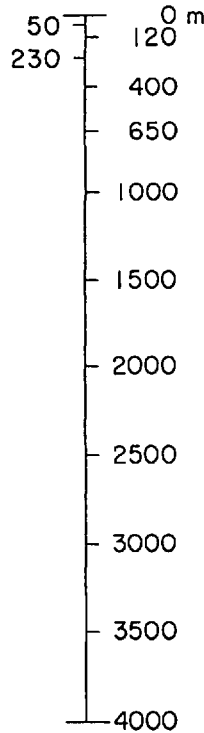


Figure 3. Vertical spacing.

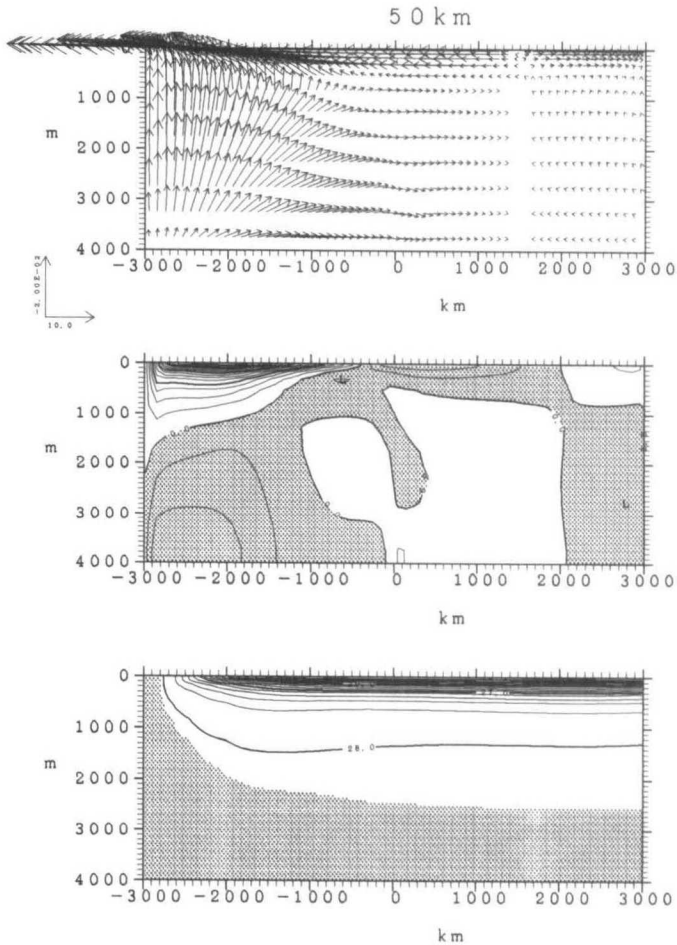


Figure 4. (a) Meridional circulation, zonal flow and density fields along the meridional sections, $x = 50$ and 1500 km (b) the zonal circulation, meridional flow and density fields along the zonal sections, $y = -1000, 0, 1000$ and 2000 km. For the zonal flow, the contour interval is 0.5 cm s^{-1} and the shaded areas indicate the westward flow. For the meridional flow, the contour interval is 0.5 cm s^{-1} and the shaded areas indicate the southward flow. For the density, the contour interval is 0.2 in σ , units, and shaded areas indicate σ , greater than 28.03 .

weighted upcurrent scheme is taken for the vertical advection term in the density equation, where the weight which is constant in the whole domain is determined empirically not to induce false increase or decrease of density at every grid point. Weaver and Sarachik (1990) pointed out that insufficient vertical resolution for the centered difference scheme sometimes leads to computational equatorial cells. Adoption of the weighted upcurrent scheme can avoid this as discussed in Sugino-hara *et al.* (1991a). Also the density grid points are located on the equator to obtain better horizontal resolution for equatorial phenomena.

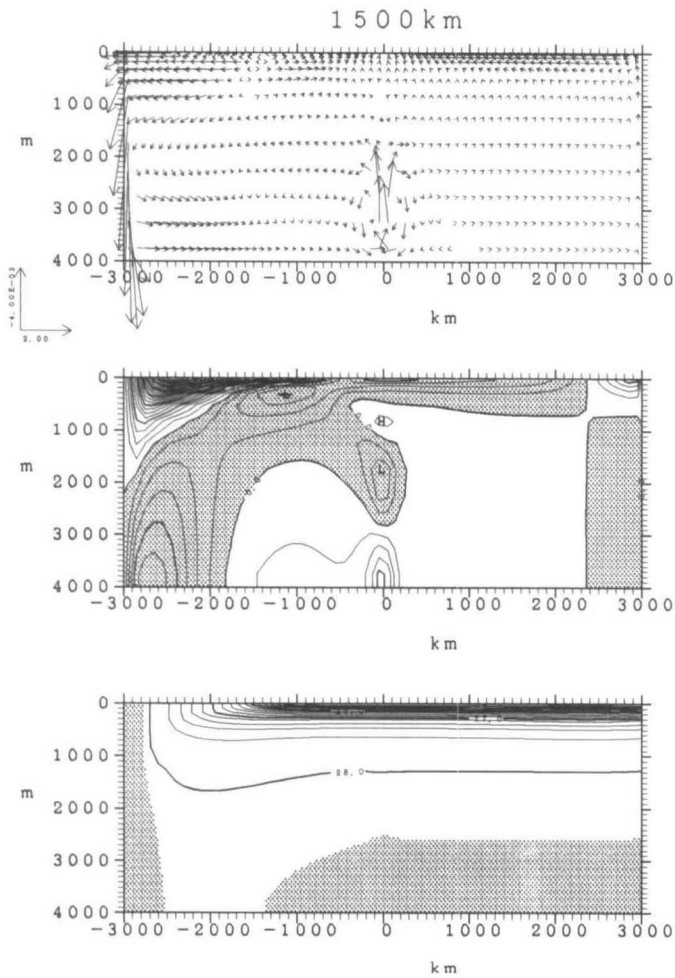


Figure 4. (Continued)

In the horizontal directions, the grid interval is taken to be 100 km. There are twelve levels in the vertical direction as shown in Figure 3. To accelerate the calculation and to reach a steady state efficiently, Bryan's accelerating method (Bryan, 1984) is adopted except in the initial transient stage. Calculations are carried out until a thermally and dynamically steady balance is established.

The following values are used for the numerical calculation: $\rho_0 = 1.0 \text{ g cm}^{-3}$; $\beta = 2 \times 10^{-13} \text{ cm}^{-1} \text{ s}^{-1}$; $K_H = 4 \times 10^7 \text{ cm}^2 \text{ s}^{-1}$, and $A_H = 8 \times 10^7 \text{ cm}^2 \text{ s}^{-1}$. The coefficients K_V and A_V are taken to be $0.2 \text{ cm}^2 \text{ s}^{-1}$ for weakly diffusive (viscous) experiments and $1.5 \text{ cm}^2 \text{ s}^{-1}$ for diffusive (viscous) experiments.

3. Result

a. Case of $K_V = A_V = 1.5 \text{ cm}^2 \text{ s}^{-1}$. Calculation was made for more than 4,000 years to entirely cover the vertical diffusion time scale. At the end of the calculation, the net

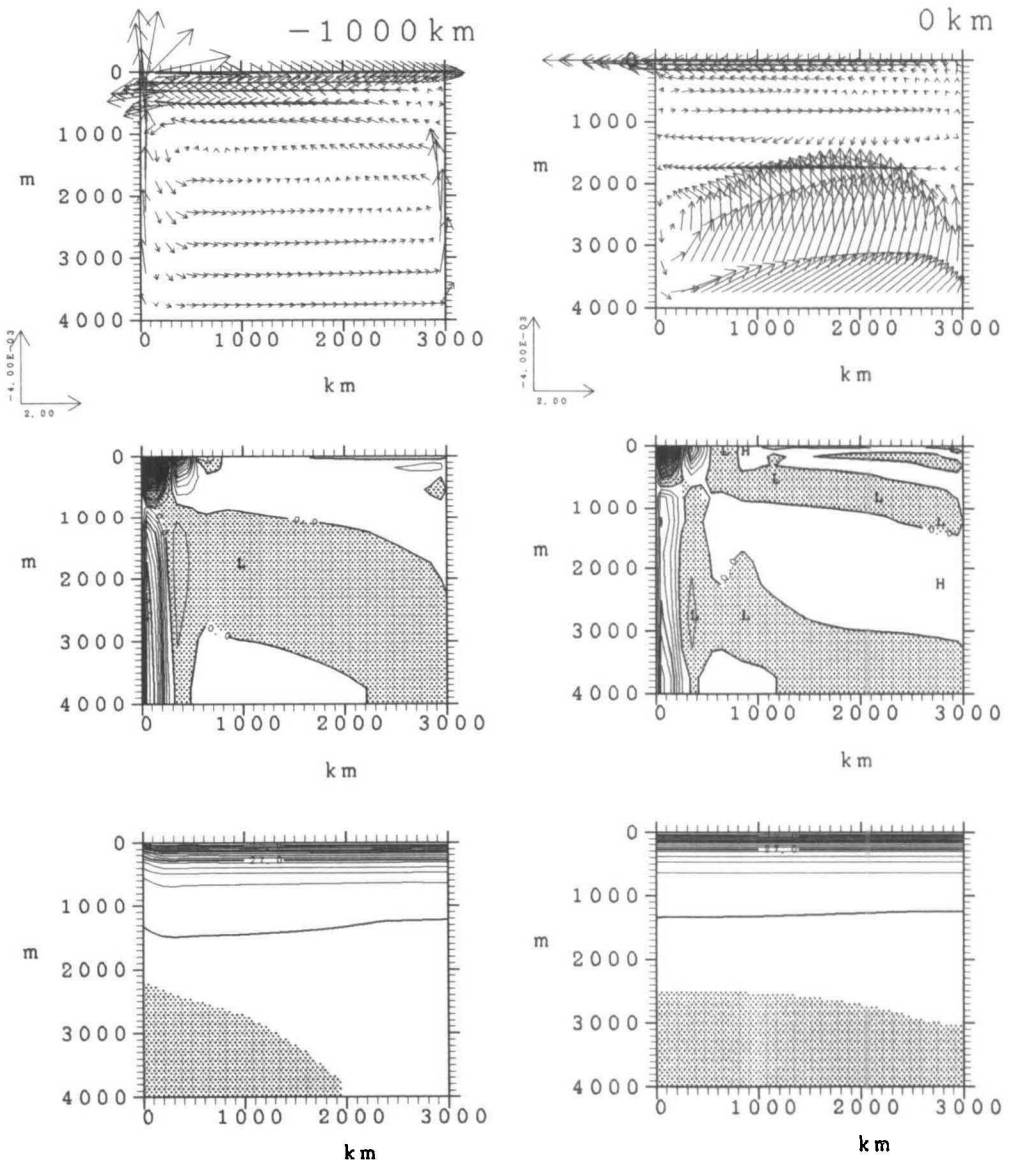


Figure 4. (Continued)

density flux through the sea surface is almost zero and no trends can be seen in density and velocity fields.

To see the basic features of the steady state solution for the present model, the density and velocity fields along the meridional sections (a) and those along the zonal sections (b) are shown in Figures 4a and b. Also plotted are the horizontal velocity fields (a) and horizontal distributions of density (b) and vertical velocity (c) in Figures 5a, b and c. As is clearly seen in the meridional sections, the heaviest water

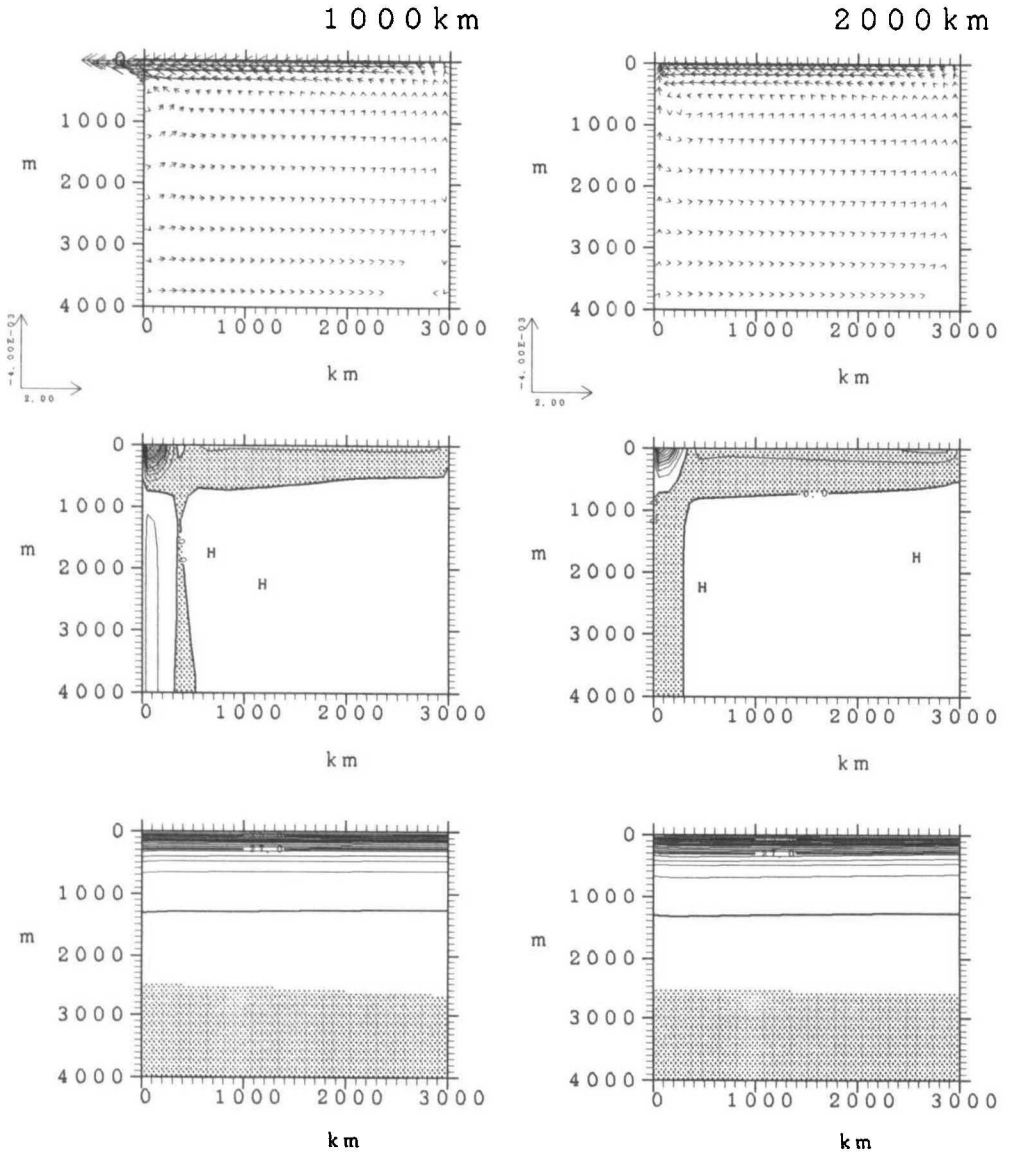


Figure 4. (Continued)

which is formed at the southern end of the ocean occupies most of the ocean basin. Above the deep water at depths shallower than 300 m the thermocline is formed and uniformly distributed except in the differential cooling region. The maximum vertical gradient of density is present at the surface and decays monotonically below.

The flow pattern at the depth 3750 m in Figure 5a represents the circulation in the lower part of the deep water (see also Figs. 4a and b). In the deep convection region where the deep water forms, the westward flow dominates and feeds the northward

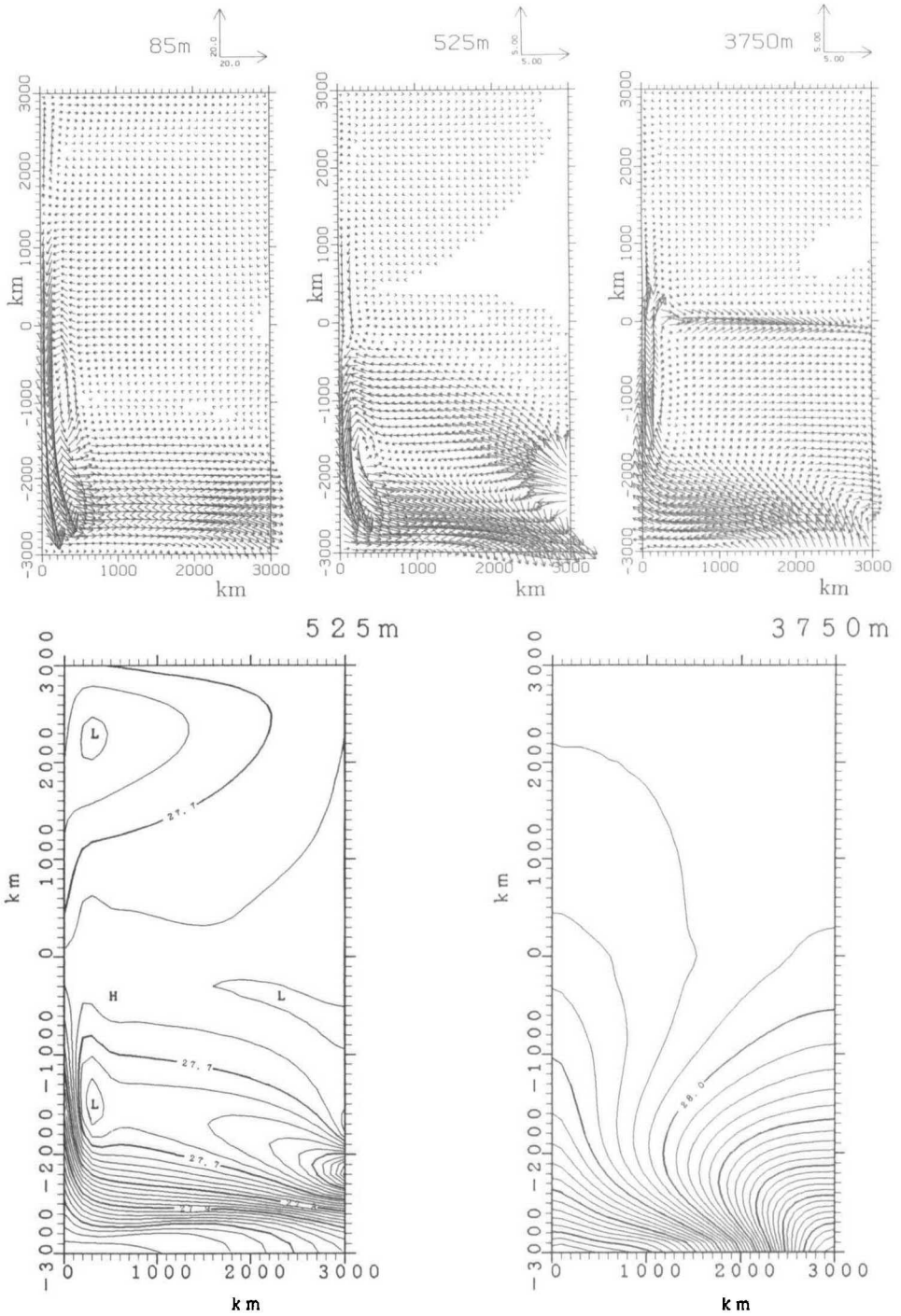


Figure 5

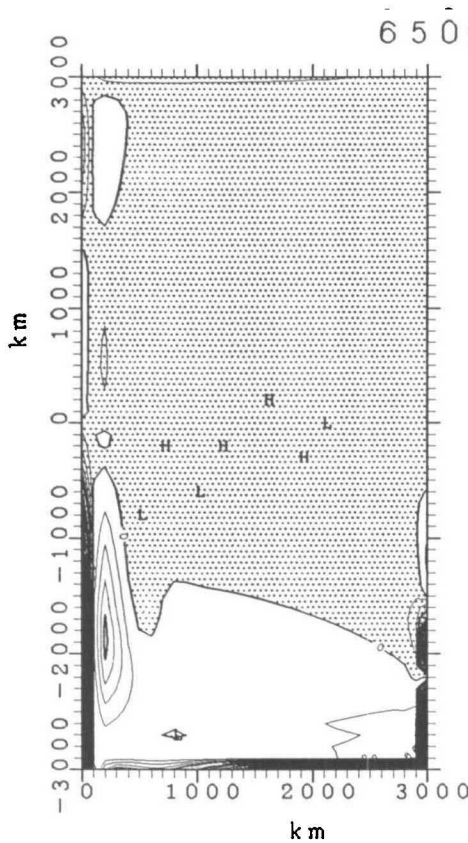


Figure 5. (a) Horizontal velocity fields at the depths 85 m, 525 m and 3750 m; (b) horizontal distribution of density at the depths 525 m and 3750 m and (c) vertical velocity at the depth 650 m. For the density the contour interval is 0.02 in σ_t , units for 525 m and 0.002 for 3750 m. For the vertical velocity, the contour interval is $5 \times 10^{-4} \text{ cm s}^{-1}$ and shaded areas indicate upwelling.

flowing western boundary current which crosses the equator feeding the interior eastward flow with the poleward component. In the northern part of the northern hemisphere, there exists a cyclonic circulation where the western boundary current flows southward. The latitude at which the northward and southward flowing western boundary currents meet is the center of the northern hemisphere. This is a case where the interior upwelling velocity is almost uniformly distributed and the flow is in geostrophic balance (Kawase, 1987). The western boundary current accompanied by the offshore countercurrent looks like that of the Munk layer type (Munk, 1950), i.e., the width is $O((A_H/\beta)^{1/3})$ and is independent of latitudes (see also Fig. 4b). The boundary current also accompanies marked vertical motions in the region close to the coast as seen in Figure 4a. That is, the northward flowing current accompanies upwelling in the southern hemisphere and downwelling in the northern hemisphere, and the southward flowing current accompanies upwelling. It also

accompanies vertical motions in the offshore region whose sense is opposite to that in the inshore region as seen in Figure 4b. The western boundary current from the southern hemisphere feeds the concentrated eastward jet along the equator at the bottom level when it crosses the equator. The horizontal distribution of density at the depth 3750 m in Figure 5b leaves traces of the way the ocean was cooled as demonstrated in SF.

In the upper part of the deep water even well below the thermocline, the flows reverse, which is clearly seen in the flow pattern at the depth 525 m in Figure 5a. This, with the meridional and zonal sections, demonstrates that the circulation in the deep water has a significant vertical structure such that the maximum upwelling in the interior occurs not within the thermocline but in the mid-depths. The southward flowing boundary current feeds the eastward flow along the equator. The horizontal field of density at the depth 525 m in Figure 5b shows that the flow is in thermal-wind balance. The circulation in the thermocline which is represented by that at the depth 85 m in Figure 5a is stronger and tends to compensate flows in the lower part of the deep water. In the deep convection region in the southern part of the basin, the eastward flow dominates and is a continuation of the southward flowing western boundary current which extends to the northern hemisphere crossing the equator and is fed by the interior westward flow with the equatorward component (see Fig. 5a). In the northern part of the northern hemisphere, there exists an anticyclonic circulation. The total transport is almost zero except in the western boundary current and the zonal jets along the equator, which reflect the fact that the motion in the interior is in geostrophic balance and satisfies the geostrophic vorticity balance, $\beta v = f \partial w / \partial z$. As seen in the horizontal distribution of the vertical velocity at the depth 650 m in Figure 5c, the vertical velocity in the interior is, in general, upward (upwelling) except in the formation region where strong downwelling occurs especially along the southern and eastern boundaries. Waters upwelled in the interior flow back to the deep convection region as the southward flowing western boundary current in the upper part of the ocean, and go down to the lower part along these boundaries. It is also seen at this depth that the western boundary current has the double structure with respect to the vertical motion.

The zonal section along the equator and also the meridional sections (Fig. 4) clearly show that a set of alternating zonal jets along the equator forms. The eastward jets are fed by the western boundary currents (see Fig. 5a). The lower westward jet is fed by the strong upwelling from below and weak downwelling from above along the equator, and the upper westward flow is fed by the interior flows (see Fig. 5a). The speed of the jets is stronger on the western side. As clearly seen in the meridional section at the center of the basin, the lower two jets are associated with a pair of small overturning cells close to the equator, i.e. the strong upwelling at the equator and downwellings on both sides of it. The meridional flow is convergent at the bottom level which is the core of the eastward jet and divergent at depth 2000 m where the core of the westward jet is. The convergence and divergence are linked by the strong upwelling all along the equator. As for the upper two jets, they are associated with

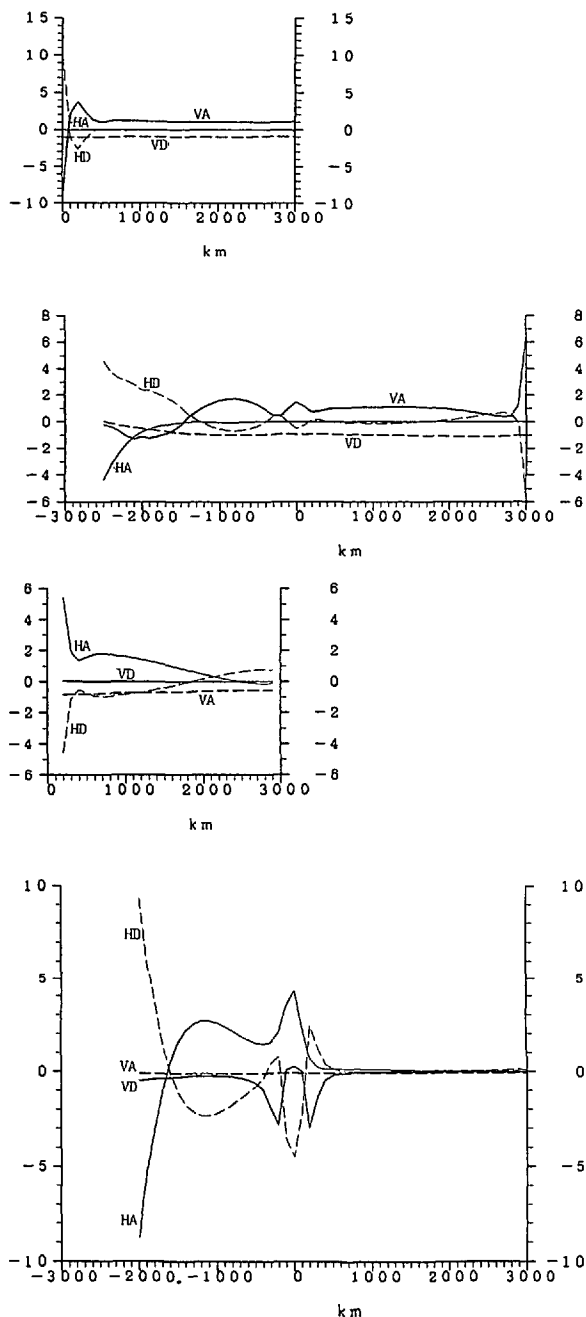


Figure 6. Terms in the density equation along $y = 1000$ km (upper) and along $x = 1500$ km (lower) at the depths 525 m (a) and 3750 m (b). HA and HD are for the horizontal advection and diffusion term, and VA and VD for the vertical advection and diffusion term. The unit of the ordinate is $10^{-9} \text{ s}^{-1} \cdot \sigma$, for the depth 525 m, and $10^{-12} \text{ s}^{-1} \cdot \sigma$, for the zonal section and $10^{-11} \text{ s}^{-1} \cdot \sigma$, for the meridional section for 3750 m.

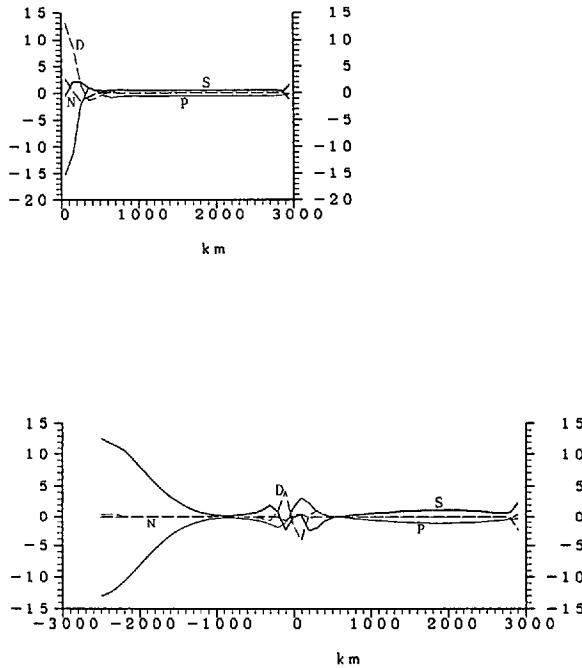


Figure 7. Terms in the vorticity balance at the depth 3250 m along $y = 1000$ km (upper) and along $x = 1500$ km (lower). P is for the planetary vorticity advection, βv , S for the vorticity stretching, $f\partial w/\partial z$, D for the horizontal diffusion of the vorticity, and N for the nonlinear terms. The unit of the ordinate is 10^{-14} s^{-2} .

convergent meridional flows. It should be remarked that there exists a marked zonal density gradient even in the deep water (see Fig. 5b).

Each of the terms in the density equation is plotted in Figures 6a and b for the zonal section in the northern hemisphere and for the meridional section at the center of the ocean at the depths 525 m (a) and 3750 m (b). For most of the interior, at the thermocline depths, the dominant balance is between the vertical diffusion and vertical advection terms, although only the advection terms dominate in the balance for the flux type representation of the density equation in SF. This balance, $w\partial\rho/\partial z = K_v\partial^2\rho/\partial z^2$ explains why the maximum upwelling occurs not within but below the thermocline. The bottom level has a different balance from that at the thermocline depths; the balance is between the horizontal advection and vertical and lateral diffusion terms. Importance of the horizontal advection is also understood when comparison is made between the flow pattern and the density distribution at the bottom level (Figs. 5a and b). The horizontal advection also plays a role at the level just above the bottom level. Near the lateral boundaries, the lateral diffusion plays an important role in the balance, which may suggest the existence of the boundary layer of Warren (1976). The vertical advection at the thermocline depths and the horizontal advection at the bottom level makes a major contribution to the balance against

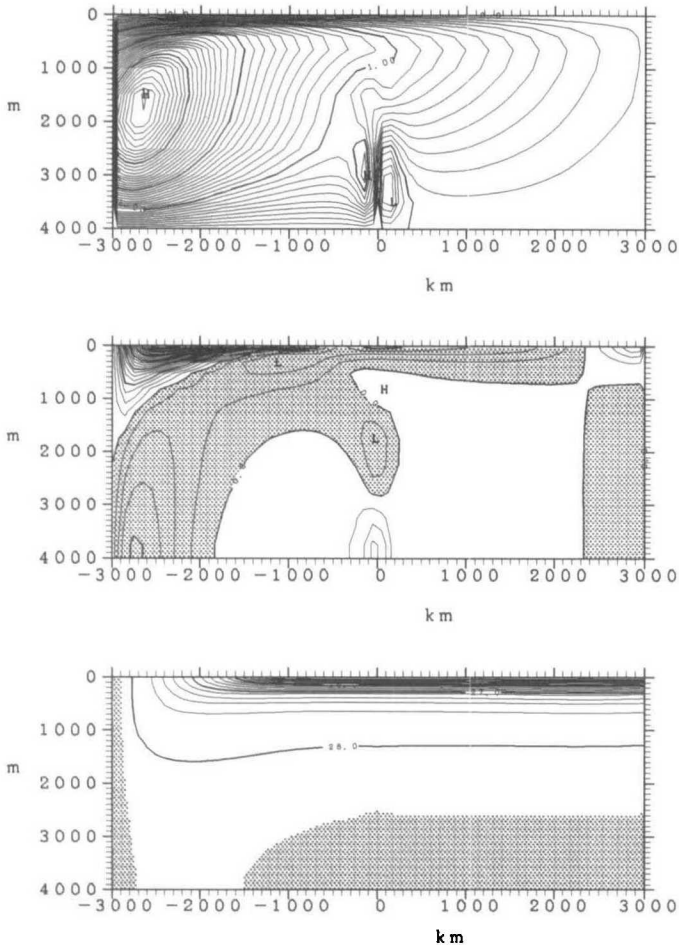


Figure 8. Streamfunction of zonal-mean circulation (upper) and zonal averages of zonal flow (middle) and density (lower). For the stream function, the contour interval is $10^{10} \text{ cm}^3 \text{ s}^{-1}$. For the zonal flow, the contour interval is 0.5 cm s^{-1} and the shaded areas indicate the westward flow. For the density, the contour interval is 0.2 in σ_t units and the shaded areas indicate σ_t greater than 28.03.

the lateral diffusion. In the equatorial region, the enhanced vertical advection and/or horizontal advection is counterbalanced by the lateral diffusion. In the southern hemisphere where the differential cooling takes place, the lateral diffusion counterbalances the enhanced vertical and horizontal advection. It is understood that the vertical diffusion plays an essential role in the whole ocean domain.

The terms in the vorticity balance at the depth 3250 m are plotted in Figure 7 along $y = 1000 \text{ km}$ and along $x = 1500 \text{ km}$. For most of the interior, the geostrophic vorticity balance, $\beta v = f \partial w / \partial z$ holds. Near the western boundary, lateral friction plays an essential role. In the equatorial region the lateral friction becomes impor-

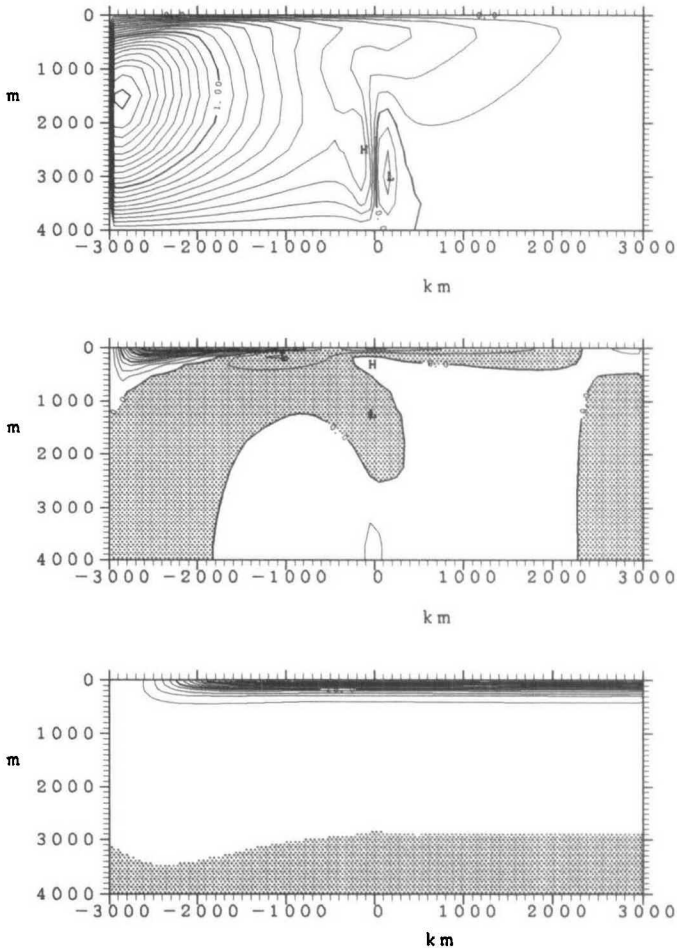


Figure 9. As in Figure 8 but for the case of $A_\nu = K_\nu = 0.2 \text{ cm}^2 \text{ s}^{-1}$. For the density the shaded areas indicate σ_t greater than 28.973.

tant. It should be remarked that the vertical friction is not important in the balance. As for the momentum balance in the equatorial region, the flow is basically in geostrophic balance except at the equator where the vertical and lateral friction counterbalances the zonal pressure gradient.

The zonally integrated continuity equation allows us to define a stream function for the meridional circulation,

$$\bar{v}L = -\frac{\partial\psi}{\partial z}, \quad \bar{w}L = \frac{\partial\psi}{\partial y},$$

where the over-bar denotes the zonal average and L is the zonal extent of the ocean. Figure 8 shows the zonal-mean meridional circulation, and zonal averages of density

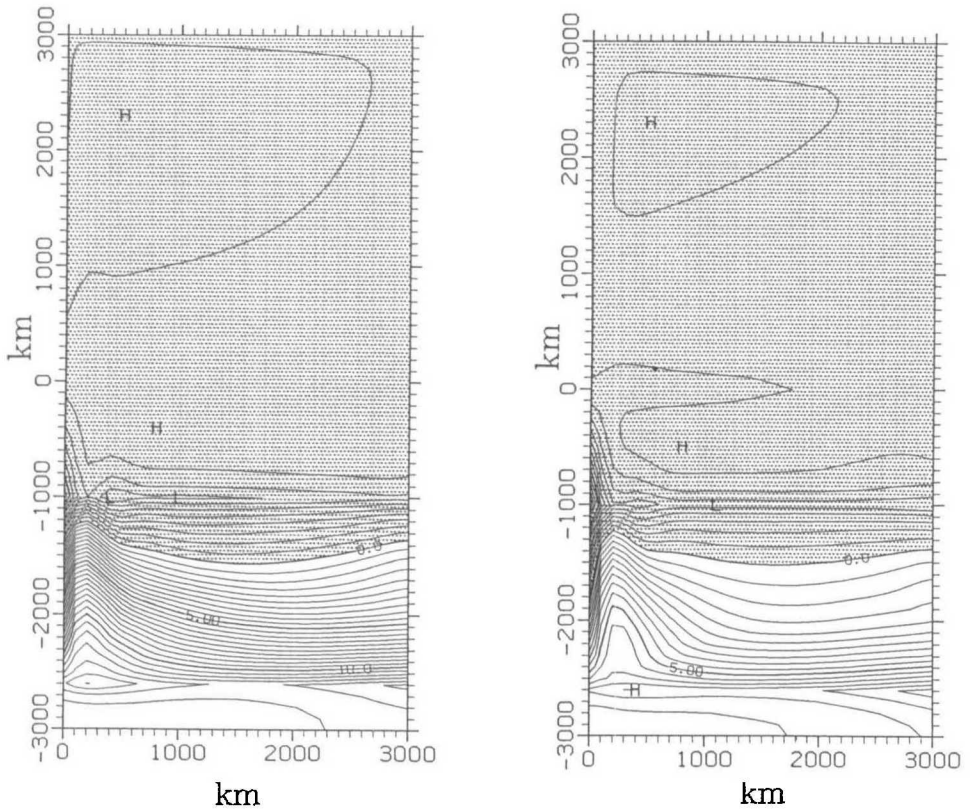


Figure 10. Horizontal distribution of the density flux through the sea surface for the case of $A_v = K_v = 1.5 \text{ cm}^2 \text{ s}^{-1}$ (left) and for the case of $A_v = K_v = 0.2 \text{ cm}^2 \text{ s}^{-1}$ (right). The contour interval is $5 \times 10^{-5} \text{ cm s}^{-1} \cdot \sigma_t$ units. Shaded areas indicate the density flux out of the ocean.

and zonal flow. Strong upwelling in the southern hemisphere is almost entirely due to the western boundary current, while the upwelling in the northern hemisphere reflects the interior flows because the western boundary current in the southern part of the northern hemisphere flows northward with marked downwelling. It is easily recognized that the pattern of the stream function represents the basic nature of the circulation induced by the surface cooling. The deep water forms in the very confined region at the southern end of the ocean and spreads toward the north gradually upwelling; there is a singularity in the equatorial region where a pair of small overturning cells form. It should be remarked that there is a southward return flow well below the thermocline. Also the zonally average fields for density and zonal flow reflect the characteristics of the thermohaline circulation (compare with Fig. 4a).

b. Case of $K_v = A_v = 0.2 \text{ cm}^2 \text{ s}^{-1}$. A calculation was made with the smaller values of the coefficients of the vertical diffusivity and viscosity. A steady state is obtained after calculation for more than 6,000 years. The meridional circulation, density and zonal

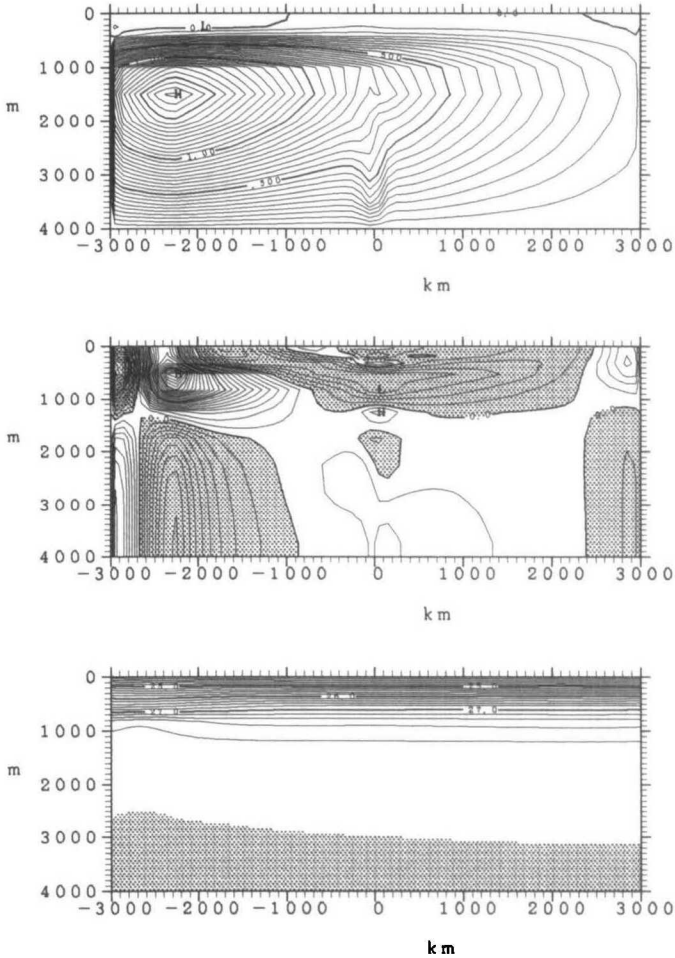


Figure 11. As in Figure 8 for the cases of the cold water formation inside the ocean. $A_\nu = K_\nu = 1.5 \text{ cm}^2 \text{ s}^{-1}$ (a) and $A_\nu = K_\nu = 0.2 \text{ cm}^2 \text{ s}^{-1}$ (b). For the stream function, the contour interval is $5 \times 10^9 \text{ cm}^3 \text{ s}^{-1}$. For the zonal flow, the contour intervals are 0.1 cm s^{-1} for (a) and 0.05 cm s^{-1} for (b) and the shaded areas indicate the westward flow. For the density, the contour interval is 0.2 in σ_t units and the shaded areas indicate σ_t greater than 27.995.

flow for the zonal averaged fields are shown in Figure 9. As expected, the deep water which is colder occupies more of the ocean basin and the thermocline is concentrated at the shallower depths. The meridional circulation and zonal flows become significantly weaker, say one half of the previous case. It should be emphasized that the flows well below the thermocline are southward even in this case. A set of alternating zonal jets along the equator also forms though the horizontal extent of the flow is smaller and the magnitude is weaker. The vertical scale of the lower two jets is larger. The pair of small overturning cells close to the equator are weaker in strength, but the relative strengths of the main and equatorial cells remain fairly stable (compare

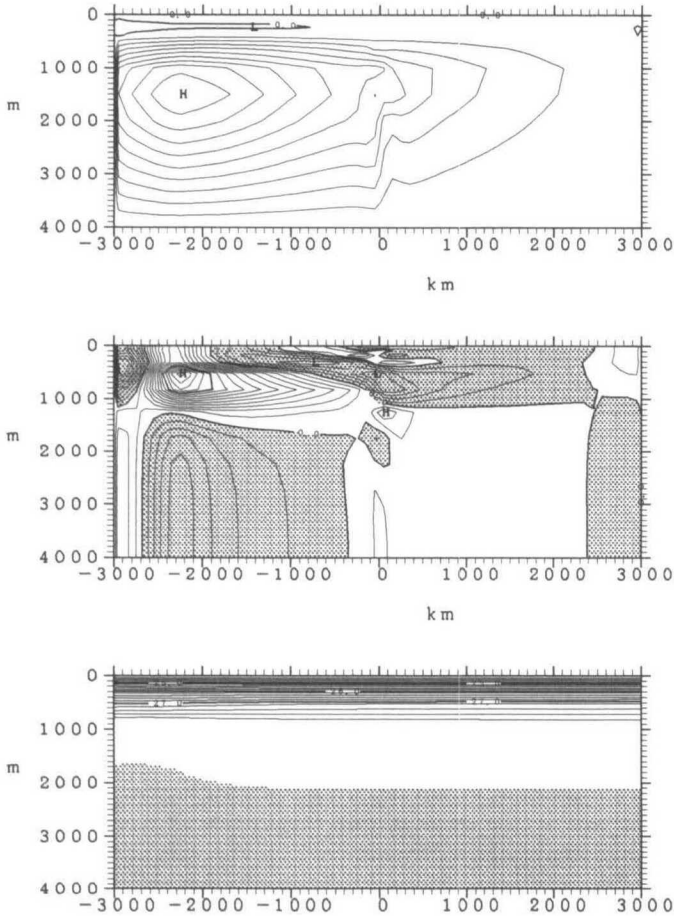


Figure 11. (Continued)

with Fig. 8). As for the density balance (not shown here), the same balance as in the previous case holds, although the magnitude of each term is smaller. The vertical diffusion plays an essential role in the whole ocean domain even in this case.

It is useful to show the horizontal distribution of the density flux through the sea surface (Fig. 10) for illustrating the efficiency of the density (also heat) transport. Although the patterns are quite similar, the magnitude for the weakly diffusive case is about half of that for the diffusive case. Therefore, as the vertical diffusivity increases, the ocean is more effectively cooled and heated through the sea surface. The thermocline deepens and the circulation becomes stronger so as to carry heat from the heating to cooling region effectively.

c. Other cases. To understand dependence on each of the vertical diffusivity and viscosity, cases where A_v is taken to be $0.2 \text{ cm}^2 \text{ s}^{-1}$ for $K_v = 1.5 \text{ cm}^2 \text{ s}^{-1}$ and A_v is taken

to be $1.5 \text{ cm}^2 \text{ s}^{-1}$ for $K_V = 0.2 \text{ cm}^2 \text{ s}^{-1}$ are also calculated. The results show that the effects of viscosity are insignificant. In fact, the results for $A_V = 0.2 \text{ cm}^2 \text{ s}^{-1}$ and $K_V = 1.5 \text{ cm}^2 \text{ s}^{-1}$ are almost same as those for $A_V = 1.5 \text{ cm}^2 \text{ s}^{-1}$ and $K_V = 1.5 \text{ cm}^2 \text{ s}^{-1}$. A set of alternating zonal jets along the equator associated with meridional circulation and the significant vertical shear in circulation well below the thermocline are the same. Thus, as was expected from the vorticity balance shown in Figure 7, the thermohaline circulation is controlled mainly by effects of vertical diffusivity, not by vertical viscosity at least within our parameter range.

The horizontal viscosity is not important for the thermohaline circulation except along the western boundary and the equator. The results of a case for $A_V = K_V = 1.5 \text{ cm}^2 \text{ s}^{-1}$, $A_H = 4 \times 10^8 \text{ cm}^2 \text{ s}^{-1}$, and $K_H = 4 \times 10^7 \text{ cm}^2 \text{ s}^{-1}$ (A_H is five times larger than the first case) show insignificant changes in circulation and density structure in the interior, while the western boundary current becomes wider and weaker in magnitude as expected for the Munk layer. The alternating zonal jets along the equator are also significantly weaker and broader though the vertical structure is not changed.

In contrast to the horizontal viscosity, the horizontal diffusivity affects the circulation and density structure especially around the deep convection region. The results of an experiment with $A_V = K_V = 1.5 \text{ cm}^2 \text{ s}^{-1}$, $A_H = 8 \times 10^7 \text{ cm}^2 \text{ s}^{-1}$ and $K_H = 2 \times 10^8 \text{ cm}^2 \text{ s}^{-1}$ (K_H is five times larger) show that the circulation pattern and density structure are significantly modified in the southern hemisphere, while those in the northern hemisphere show very small changes. A set of alternating zonal jets along the equator also forms though it looks more like that for the case of weak vertical diffusivity. In summary, it may be concluded that the thermohaline circulation is controlled mainly by the effect of the diapycnal mixing, and a set of alternating zonal jets along the equator and the significant vertical shear in circulation well below the thermocline are important ingredients of the thermohaline circulation.

d. Cases where the cold water is formed inside the ocean. Cases where the cold water is formed inside the ocean as in SF are also calculated. The cold water formation is made at depths deeper than 650 m in the southern part of the southern hemisphere by including a mass source term which is proportional to $(\rho_c - \rho)$ in the density equation, where ρ_c is the reference density and is taken to be 28.0 in σ_t units (for the details, see SF). At the sea surface, the reference density for heating is set to be constant, 24.0 in σ_t units. The zonal averaged fields for cases of $K_V = A_V = 1.5 \text{ cm}^2 \text{ s}^{-1}$ and $K_V = A_V = 0.2 \text{ cm}^2 \text{ s}^{-1}$ are shown in Figures 11a and b, respectively. As expected, with increasing diffusivity, the thermocline tends to spread down to the deeper depths, i.e., depths deeper than the top of the cold water formation, and the meridional circulation and zonal flows become stronger. The waters in the thermocline flow southward and the depth of the maximum vertical velocity is well below the thermocline. That is, meridional circulation tends to be confined at depths below the top of the cold water formation. This feature may be understood as follows. The ocean is uniformly heated through the sea surface, which leads to no horizontal distribution of density, hence no motion near the surface. At the deeper levels

introduction of cold water leads to creation of horizontal density contrasts and hence circulation since the cold water is formed on one side of the ocean and is subjected to vertical diffusion. It should be remarked that in the density balance, the vertical diffusion plays an essential role in the whole ocean domain. For the surface cooling case, the same things occur, although the thermal structure caused by vertical diffusion between the sea surface and the top of the cold water changes its shape into the upper thermocline. It is concluded that the significant vertical shear below the thermocline is an essential nature of the thermohaline circulation.

4. Discussion

a. Nature of the thermohaline circulation. Here we discuss the basic nature of the steady thermohaline circulation as horizontal convection on a β -plane. Suppose that the sea water is an ideal fluid, i.e. a nonviscous and nondiffusive fluid. Further, consider a case where the cold water is formed inside the ocean in the southern part of the southern hemisphere just like we did in 3d. For this case, it is intuitively understood that the depths deeper than the top of the deep water formation are occupied by the deep water and no circulation exists. Next, let the depths for the cold water formation thicken so as to cool the whole depths. Then the whole of the ocean is occupied by the cold water and again no motion exists. We extend this intuition to the case where the ocean is heated and cooled through the sea surface. Although no heat enters and exits without diffusion, the convective overturning process can take place in the cooling region (if any small diffusion exists). This overturning process corresponds to the cold water formation in the whole depths, then, we can easily imagine that the ocean basin is occupied by the cold water except the top thin shear layer and is motionless. In short, for an almost ideal fluid ocean, the ocean tends to be occupied by the coldest water formed in the deep convection region and to be at rest, even when differential cooling at the sea surface, however it is distributed, is imposed. Therefore it is understood that it is essential for the ocean water to be a nonideal fluid to have significant motions.

b. A set of alternating zonal jets along the equator. The equatorial radius of deformation for the vertical modes lower than the eighth obtained in the present experiment is larger than the horizontal grid size, 100 km. Suginohara *et al.* (1991a) calculated a case where the vertical resolution is doubled for the deep water and obtained a set of alternating zonal jets along the equator whose structure is not changed. Thus the horizontal and vertical grid sizes used in the present model yield sufficient resolution for the jets and associated meridional circulation.

For all of the cases studied in the present paper, three zonal jets form below the thermocline. Thickness, width and strength are different among the cases. The width of the jets is basically related to the equatorial radius of deformation of several vertical modes which is determined by the global thermohaline circulation. The vertical modal structure of the horizontal flow in the off-equator region apparently

takes that of the first baroclinic mode. However, close examination of the modal structure of the western boundary current in the southern hemisphere shows that it consists of many higher modes. Changes in this modal structure seem to yield those in thickness and width of the jets.

A simple explanation for the formation of a set of alternating zonal jets (stacked jets) along the equator may be possible if pre-existence of the stratification is assumed and superposition of the results for a single vertical mode model like Kawase's (1987) is made. For the single mode model, he showed that damping of Rossby and Kelvin waves leads to the eastward jet along the equator when the Newtonian cooling works effectively. For simplicity, consider a two-mode model where the lower mode has a very high wave speed and the higher mode a very low speed. For the western boundary current in the southern hemisphere, we assume that it consists of two modes but the lower mode motion dominates as was found in the present model. We further assume that we may be able to take parameters such that significant wave damping takes place for the higher mode but not for the lower mode in the equatorial region. For the lower mode response, there are insignificant flows along the equator due to insignificant wave damping, while for the higher mode response, significant wave damping occurs, and zonal jets are formed along the equator. Consequently, we observe predominance of the higher mode motion along the equator. Thus, the formation of the stacked jets may be a necessary consequence of the selective damping for the vertical higher mode waves.

A pair of overturning cells associated with the stacked jets occurs all the way along the equator. The meridional flow is convergent at the bottom level which is the core of the eastward jet and divergent at the depth where the core of the westward jet is. The convergence and divergence are linked by an upwelling flow all along the equator. The result that the eastward jet is associated with convergent meridional flows all along the equator yields a marked difference from experiments using an inverted reduced gravity model (Kawase, 1987). From case-studies where wider range of parameters such as the equivalent depth and vertical diffusivity and viscosity coefficients are considered and the horizontal diffusivity and viscosity are newly included, it is shown that the eastward jet is always associated with divergent meridional flows. The difference may be because in the present multi-level model a marked zonal density gradient along the equator is created, and in fact the eigenvalue for the vertical modes higher than the seventh is several tens percent different between the western and eastern sides along the equator. The associated geostrophic flows just outside the equator are equatorward. Therefore, prescribing the basic stratification may not be appropriate for modeling details of the stacked jets and associated meridional circulation.

Here we also give an intuitive explanation for the formation of the stacked jets along the equator following the set-up experiment of SF. Consider an ideal fluid ocean forced by the body cooling in 3d (see Fig. 12). First, it is noted that as discussed in 4a, at the steady state, the depths deeper than the top of the cold water formation are occupied by the cold water, and no circulation exists. Next, we consider a set-up

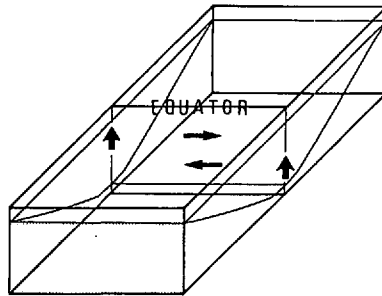


Figure 12. Schematic view for formation process of a set of alternating zonal jets along the equator. The shaded area is for the cold water formation. At the steady state the depths deeper than the top of the cold water formation are occupied by the cold water. The curves represent the top of the depths where the cold water is introduced only by the density currents which tend to conserve potential vorticity. The arrows indicate the movement of the cold water introduced into the upper levels by the upwelling at the eastern boundary.

process. As studied in SF, introduction of the cold water into the ocean is performed by the Kelvin and Rossby wave-type density currents which tend to conserve potential vorticity, i.e., $(\zeta + f)/h$ in a layer-model expression, where ζ is relative vorticity which is only for resolving singularity at the equator and h the thickness of the cold water. Due to this constraint, the cold water introduced by the density currents cannot occupy whole of the domain attained at the steady state. Our problem is how the rest of the domain is occupied by the cold water. SF clearly demonstrated that when the equatorial Kelvin wave-type density current hits the eastern boundary, upwelling occurs. By this upwelling, the cold water is introduced into the upper levels and flows to the west along the equator. Then at the western boundary, the upwelling occurs, and the cold water is introduced into further upper levels and flows to the east. And the Rossby dispersion follows, and occupation of the whole domain by the cold water is completed. When the effect of vertical diffusion is taken into consideration, damping of the equatorial Kelvin and Rossby waves leads to the existence of the zonal pressure gradient along the equator even at the steady state. Therefore, it may be said that a set of alternating zonal jets along the equator is a reminiscence of the set-up process.

As for the equatorial undercurrent, McCreary (1981) showed that the effect of the vertical diffusivity is essential for the formation, and higher baroclinic modes contribute to the current. But, in spite of the simplicity in forcing mechanism and the prescribed basic stratification, detailed sensitivity of the vertical and horizontal scales of the current to the diffusivity was not clarified. In the present model, the stacked jets are associated with the thermal structure in the equatorial region which itself is determined by the global thermohaline circulation. Therefore, it is really a difficult problem to clarify details of its dynamics. However, we believe that a set of alternating zonal jets along the equator is a realistic feature and is an essential nature of the thermohaline circulation.

c. Deep western boundary current. The deep western boundary current accompanied by the offshore countercurrent looks like that of the Munk layer type, i.e., the width is $O((A_H/\beta)^{1/3})$ and is independent of latitudes. However, it accompanies significant vertical motions. For example, the northward flowing current in the southern hemisphere accompanies upwelling on the inshore side and downwelling on the offshore side. This double structure with respect to vertical motion has a resemblance with that obtained by Warren (1976) where effects of the lateral diffusion play an essential role. But, for the horizontal flows no countercurrent exists in Warren's model. This difference may be explained by the work of Masuda and Uehara (1991) where characteristics of the boundary layer are examined using a reduced gravity model with horizontal diffusion and viscosity. They classify the dynamics of the boundary layer into viscous and diffusive regimes. In both regimes, the lateral diffusion dominates to determine the distribution of vertical velocity. The criterion dividing the two regimes is given by

$$\left(\frac{3A_H}{K_H}\right)^{1/2} L_R = \left(\frac{2A_H}{\beta}\right)^{1/3},$$

where L_R denotes the radius of deformation. When the left-hand side is larger than the right-hand side, the boundary layer is in the viscous regime. For this regime, the boundary current accompanies the offshore countercurrent, and an intense vertical motion in a narrow layer adjacent to the coast and an opposite vertical motion on the offshore side take place. The width is close to that of the Munk layer. In contrast, when the left-hand side is smaller than the right-hand side, the boundary layer is in the diffusive regime. This is the layer which Warren (1976) obtained, i.e., the boundary current accompanies no countercurrent. In the present model, as discussed in 4b, the gravest baroclinic mode motions dominate, and this yields a boundary layer of the viscous regime, i.e. the deep western boundary current accompanied by the offshore countercurrent and a double structure for the vertical motion. It is noted that in addition to motions associated with the first baroclinic mode, we can observe characteristics of the diffusive regime for the higher modes in Figure 4b.

For the results obtained in the present model, the inshore boundary layer may be too narrow and vertical motion there may be too strong to be realistic. As was pointed out by Veronis (1975) and Warren (1976), this is due to the fact that the tilt of isopycnals associated with the boundary current yields strong diapycnal mixing. A quantitative estimate of these features requires further studies on oceanic mixing.

The occurrence of the interior downwelling in Holland's model (1971) is surely due to effects of horizontal diffusion as was discussed by Veronis (1975). But, the interior downwelling is not a motion associated with the boundary layer. Masuda and Uehara (1991) clearly demonstrated that cold water formation situated at the northeast corner of the basin leads to the interior downwelling when effects of the horizontal diffusion are dominant.

5. Concluding remarks

The steady buoyancy-driven circulation forced by the concentrated cooling and broad heating at the sea surface has been investigated using multi-level numerical models. As already demonstrated (Bryan, 1987; SF; and Colin de Verdière, 1988), the circulation and associated thermal structure strongly depend upon the effect of the vertical diffusivity. As the vertical diffusivity increases, the ocean is more effectively cooled and heated through the sea surface, and consequently the thermocline deepens and the circulation becomes stronger to effectively carry heat from the heating to cooling regions. In the limit of an ideal fluid, no influx and efflux of heat through the sea surface takes place and no motion exists. It can be said that the steady buoyancy-driven circulation is maintained by the effect of the vertical diffusion. The effects of advection and lateral diffusion serve to remove the horizontal density gradient and therefore to slow down the circulation; the latter is driven by the horizontal gradient which is maintained only by the vertical diffusion. Thus, in the thermodynamic balance, the vertical diffusion plays an essential role in the whole ocean domain. In counterbalancing vertical diffusion, horizontal advection at the deepest levels and vertical advection in the rest of the interior region plays a dominant role. Thus, horizontal transport of the cold water from the convective (cooling) to the diffusive (heating) region is made mainly in the lowest part of the deep water. This may be due to the fact that the water at the deepest levels is subjected only to heating from above by the vertical diffusion since the ocean bottom prohibits vertical motion and is thermally insulated. The significant shear in the deep circulation is a necessary consequence of the predominance of vertical diffusion. Thus the Stommel and Arons pattern for the deep circulation tends to be confined to the lower part of the deep water, which is consistent with the fact that the stratification forms from the deepest part of the ocean to shallower depths as demonstrated in SF.

In the present model, a set of alternating zonal jets along the equator predicted in SF has been reproduced, and details of the jets and associated meridional circulation have been clearly demonstrated. Direct current measurements in the equatorial Pacific show that a set of alternating zonal jets exists and these jets are steady (Firing, 1989). The distribution of Freon in the equatorial Atlantic (Weiss *et al.*, 1985 and Weiss, personal communication) cannot be accounted for without the existence of these jets.

In the present experiment, to simplify the model, differential cooling which is distributed over the whole ocean surface is not considered. As long as the deep water is not formed in other regions, the circulation and thermal structure below the mid-thermocline are essentially the same, even when differential cooling over the whole ocean is taken into account (Suginohara *et al.*, 1991b).

The present study ignored effects of wind stresses, i.e. the surface gyres. Distributions of the wind stresses cause deformation of the thermocline and lead to a realistic thermal structure (Suginohara *et al.*, 1991b). However, as demonstrated in the

present study, the formation of the thermocline as a characteristic feature of the ocean thermal structure is performed by the differential cooling through the sea surface. Effects of the wind stresses deform it.

Acknowledgments. We would like to acknowledge Drs. Kinjiro Kajiura, Akira Masuda, Taroh Matsuno and Masao Fukasawa for pleasant and fruitful discussions. Thanks are extended to Dr. George Veronis for helpful comments.

REFERENCES

- Bryan, F. 1987. Parameter sensitivity of primitive equation general circulation models. *J. Phys. Oceanogr.*, *17*, 970–985.
- Bryan, K. 1984. Accelerating the convergence to equilibrium of ocean-climate models. *J. Phys. Oceanogr.*, *14*, 666–673.
- Colin de Verdière, A. 1988. Buoyancy driven planetary flows. *J. Mar. Res.*, *46*, 215–265.
- Firing, E. 1989. Mean zonal currents below 1500 m near the equator, 159W. *J. Geophys. Res.*, *94*, 2023–2028.
- Holland, W. R. 1971. Ocean tracer distributions. Part I. A preliminary numerical experiment. *Tellus*, *23*, 371–392.
- Kawase, M. 1987. Establishment of mass-driven abyssal circulation. *J. Phys. Oceanogr.*, *17*, 2294–2317.
- Masuda, A. and K. Uehara. 1991. A reduced-gravity model of the abyssal circulation with Newtonian cooling and horizontal diffusion. *Deep-Sea Res.*, (submitted).
- McCreary, J. P. 1981. A linear stratified ocean model of the equatorial undercurrent. *Phil. Trans. Roy. Soc. London*, *A298*, 603–635.
- Munk, W. H. 1950. On the wind driven ocean circulation. *J. Meteor.*, *7*, 79–93.
- Rosby, H. T. 1965. On the thermal convection driven by nonuniform heating below: An experimental study. *Deep-Sea Res.*, *12*, 9–16.
- Stommel, H. 1962. On smallness of sinking regions in the ocean. *Proc. Nat. Acad. Sci. U.S.A.*, *48*, 766–772.
- Stommel, H. and A. B. Arons. 1960. On the abyssal circulation of the world ocean-II. An idealized model of the circulation pattern and amplitude in oceanic basins. *Deep-Sea Res.*, *6*, 217–233.
- Suginohara, N., S. Aoki and M. Fukasawa. 1991a. Effects of buoyancy flux and wind-stress on main thermocline. *J. Oceanogr. Soc. Japan*, (to be submitted).
- 1991b. Comments on “On the importance of vertical resolution in certain oceanic general circulation models.” *J. Phys. Oceanogr.*, (in press).
- Suginohara, N. and M. Fukasawa. 1988. Set-up of deep circulation in multi-level numerical model. *J. Oceanogr. Soc. Japan*, *44*, 315–336.
- Veronis, G. 1975. The role of models in tracer studies. *Symposium on Numerical Methods in Oceanography*. National Academy of Science, 133–146.
- Warren, B. A. 1976. Structure of deep western boundary currents. *Deep-Sea Res.*, *23*, 129–142.
- Weaver, A. J. and E. S. Sarachik. 1990. On the importance of vertical resolution in certain ocean general circulation models. *J. Phys. Oceanogr.*, *20*, 600–609.
- Weiss, R. F., J. L. Bullister, R. H. Gammon and M. J. Warner. 1985. Atmospheric chlorofluoromethanes in the deep equatorial Atlantic. *Nature*, *314*, 608–610.